Math. J. Okayama Univ. **62** (2020), 179–195

ANALYTIC EXTENSION OF EXCEPTIONAL CONSTANT MEAN CURVATURE ONE CATENOIDS IN DE SITTER 3-SPACE

S. Fujimori, Y. Kawakami, M. Kokubu, W. Rossman, M. Umehara and K. Yamada

Abstract. Catenoids in de Sitter 3-space S^3_1 belong to a certain class of space-like constant mean curvature one surfaces. In a previous work, the authors classified such catenoids, and found that two different classes of countably many exceptional elliptic catenoids are not realized as closed subsets in S^3_1. Here we show that such exceptional catenoids have closed analytic extensions in S^3_1 with interesting properties.

1. Introduction.

We denote by S^3_1 the de Sitter 3-space, which is a simply-connected Lorentzian 3-manifold with constant sectional curvature 1. Let $\boldsymbol{R}^4_1$ be the Lorentz-Minkowski 4-space with the metric $\langle\ ,\ \rangle$ of signature $(-+++)$. Then

$$S^3_1 = \{X \in \boldsymbol{R}^4_1\,;\, \langle X, X\rangle = 1\}$$

with metric induced from $\boldsymbol{R}^4_1$. We identify $\boldsymbol{R}^4_1$ with the 2×2 Hermitian matrices Herm(2) by

$$(t,x,y,z) \longleftrightarrow \begin{pmatrix} t+z & x+\mathrm{i}y \\ x-\mathrm{i}y & t-z \end{pmatrix},$$

where $\mathrm{i}=\sqrt{-1}$. Then S^3_1 is represented as

$$S^3_1 = \{X \in \mathrm{Herm}(2)\,;\, \det X = -1\} = \{a e_3 a^*\,;\, a \in \mathrm{SL}(2,\boldsymbol{C})\},$$

where $a^* := {}^t\overline{a}$ is the conjugate transpose of a, and

$$e_3 := \begin{pmatrix} 1 & 0 \\ 0 & -1 \end{pmatrix}.$$

To draw surfaces in S^3_1, we use the *stereographic hollow ball model* given in [4] as follows:

$$(1)\quad \mathit{\Pi} : S^3_1 \ni (t,x,y,z) \longmapsto \frac{1}{\delta}(x,y,z) \in \boldsymbol{R}^3 \quad \left(\delta := t + \sqrt{t^2+x^2+y^2+z^2} = t + \sqrt{2t^2+1}\right).$$

Mathematics Subject Classification. 53A10, 53A35; 53C50.

Key words and phrases. constant mean curvature, de Sitter space, analytic extension.

This projection Π is the composition of central projection of S^3_1 to the unit sphere S^3 centered at the origin in $\boldsymbol{R}^4$ and usual stereographic projection of S^3 into $\boldsymbol{R}^3$ from $(0,0,0,-1)$. The image of Π is the set

$$\mathcal{D}^3 := \left\{\xi \in \boldsymbol{R}^3\,;\, \sqrt{2}-1 < |\xi| < \sqrt{2}+1\right\}, \tag{2}$$

where $|\xi| := \sqrt{\xi_1^2+\xi_2^2+\xi_3^2}$ for $\xi = (\xi_1,\xi_2,\xi_3)$.

In [1], the authors classified all *catenoids* in S^3_1 (i.e. weakly complete constant mean curvature one surfaces in S^3_1 of genus zero with two regular ends whose hyperbolic Gauss map is of degree one). There are three types of catenoids:

- elliptic catenoids,
- the parabolic catenoid, and
- hyperbolic catenoids.

Parabolic catenoids have only one congruence class, whose secondary Gauss map is given by

$$g = \frac{1+\log z}{-1+\log z},$$

and they are rotationally symmetric surfaces with one cone-like singular point and two embedded ends. On the other hand, the secondary Gauss maps of hyperbolic catenoids are of the form

$$g = \frac{g_0 - \mathrm{i}}{g_0+\mathrm{i}}, \qquad g_0 := \exp((m+\mathrm{i}\tau)\log z) = z^{m+\mathrm{i}\tau},$$

where m is a non-negative integer, and τ is a non-zero real number. When $m \neq 0$ (resp. $m = 0$), hyperbolic catenoids admit only cuspidal edge singularities (resp. cone-like singular points), see [1, Page 36]. Recently, in a joint work with Seong-Deog Yang, the authors [2] proved that all hyperbolic catenoids do not admit any analytic extension.

On the other hand, there are many subclasses of elliptic catenoids, whose secondary Gauss maps g are given by

(i) $g = z^\alpha \quad (0 < \alpha < 1)$,
(ii) $g = z^\alpha \quad (\alpha > 1)$,
(iii) $g = z^m + c \quad (m = 2,3,\dots)$ with $c \in (0,\infty)\setminus\{1\}$,
(iv) $g = z^m + 1 \quad (m = 2,3,\dots)$,
(v) $g = (z^m-1)/(z^m+1) \quad (m = 2,3,\dots)$.

Except for the two cases (iv) and (v), all elliptic catenoids are closed subsets of S^3_1, since the singular sets of catenoids of type (i)–(iii) are compact. In this paper, we call the catenoids in the class (iv) (resp. (v)) *exceptional catenoids of type I* (resp. *exceptional catenoids of type II*) and we study these two classes.

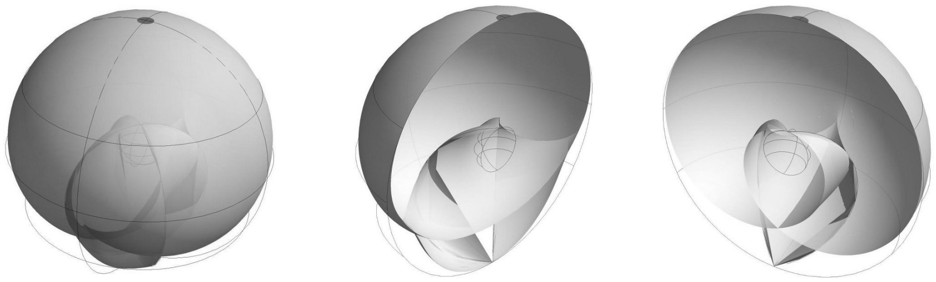

FIGURE 1. The image of f_2^{I} (left) and halves of it (center and right).

For each $m = 2, 3, \ldots,$ we set

$$F_m^{\mathrm{I}} := \frac{z^{-\frac{m+1}{2}}}{2\sqrt{m}} \begin{pmatrix} (m+1)z & z\big((m-1)z^m - m - 1)\big) \\ m-1 & (m+1)z^m - m + 1 \end{pmatrix} \tag{3}$$

and

$$F_m^{\mathrm{II}} := \frac{z^{-\frac{m+1}{2}}}{2\sqrt{2m}} \begin{pmatrix} z\big((1-m)z^m + m + 1\big) & z\big((m-1)z^m + m + 1\big) \\ -(m+1)z^m + m - 1 & (m+1)z^m + m - 1 \end{pmatrix}. \tag{4}$$

The maps $f_m^{\mathrm{J}} : \boldsymbol{C} \setminus \{0\} \to S_1^3$ defined by

$$f_m^{\mathrm{J}} := F_m^{\mathrm{J}} e_3 (F_m^{\mathrm{J}})^* \qquad (\mathrm{J} = \mathrm{I}, \mathrm{II})$$

give the exceptional catenoids. These expressions are obtained by shifting m to $m-1$ in [1, Prop. 4.9]. We will show that the image of each f_m^{J} ($\mathrm{J} = \mathrm{I}, \mathrm{II}$) has an analytic extension $\mathcal{C}_m^{\mathrm{J}}$ which is a closed set in S_1^3.

A subset $\mathcal{A}$ of a manifold M^n is called *almost embedded* (resp. *almost immersed*) if there is a discrete subset D of $\mathcal{A}$ such that $\mathcal{A} \setminus D$ is the image of an embedding (resp. an immersion) of a manifold into M^n. For example (cf. [1]),

- catenoids of class (iii) are not almost immersed,
- catenoids of class (i) are almost immersed, but not almost embedded,
- catenoids of class (ii) are almost embedded.

In Section 2, we investigate the geometric properties of f_m^{I}, and show that the image of each f_m^{I} has an analytic extension whose image is immersed outside of a compact set. See Figures 1, 2, 3, where f_2^{I}, $\mathcal{C}_2^{\mathrm{I}}$ and $\mathcal{C}_3^{\mathrm{I}}$ are drawn in the stereographic hollow ball model (1). In Section 3, we show that each $\mathcal{C}_m^{\mathrm{II}}$ can be realized as a warped product of a certain trochoid and hyperbola. In particular, $\mathcal{C}_2^{\mathrm{II}}$ and $\mathcal{C}_3^{\mathrm{II}}$ are almost embedded, and $\mathcal{C}_m^{\mathrm{II}}$ ($m \geq 4$) are almost immersed (cf. Section 3). See Figures 4, 5, where f_2^{II}, $\mathcal{C}_2^{\mathrm{II}}$ and $\mathcal{C}_3^{\mathrm{II}}$ are drawn in the stereographic hollow ball model (1) as well.

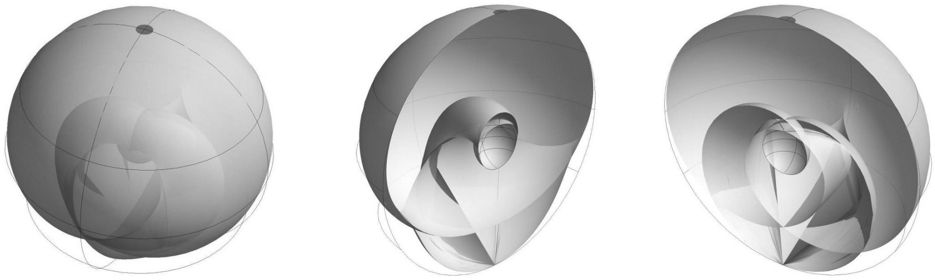

FIGURE 2. The set $\mathcal{C}_2^{\mathrm{I}}$ (left) and halves of it (center and right).

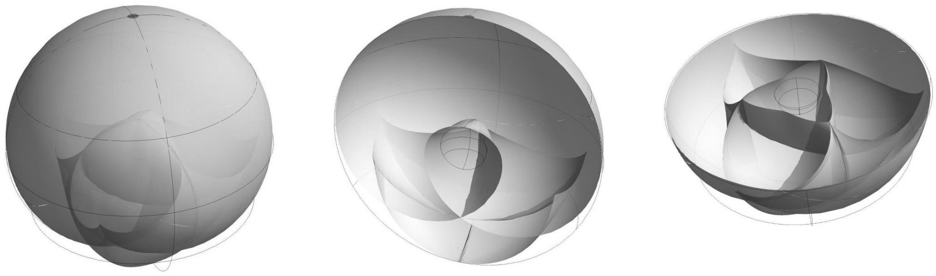

FIGURE 3. The set $\mathcal{C}_3^{\mathrm{I}}$ (left) and halves of it (center and right).

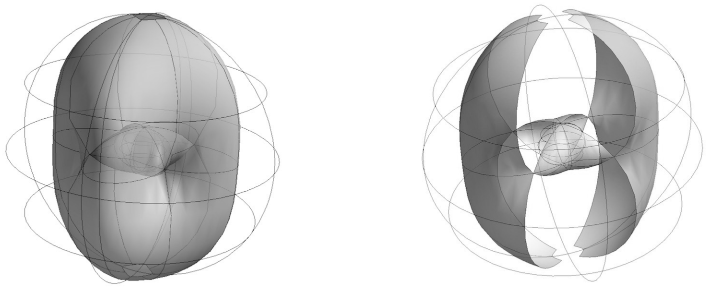

FIGURE 4. The set $\mathcal{C}_2^{\mathrm{II}}$ (left) and the image of f_2^{II} (right).

It is well-known that the de Sitter space S_1^3 can be compactified by including two spheres $\partial_\pm S_1^3$. These two sets $\partial_\pm S_1^3$ are called the *ideal boundaries*. In the stereographic hollow ball model, the relations

$$\partial_\pm S_1^3 = \{\xi \in \boldsymbol{R}^3\,;\, |\xi| = \sqrt{2} \mp 1\} \tag{5}$$

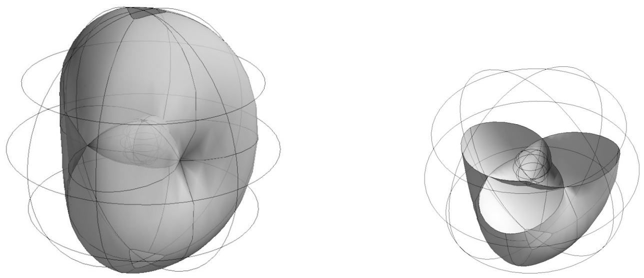

FIGURE 5. The set $\mathcal{C}_3^{\mathrm{II}}$ and half of it.

hold (cf. (2)). If a subset $\mathcal{A}$ of S_1^3 is closed, then each element of the set

$$\overline{\Pi(\mathcal{A})} \cap \partial\mathcal{D}^3 \ (\subset \partial_- S_1^3 \cup \partial_+ S_1^3)$$

is called an *endpoint*, where $\overline{\Pi(\mathcal{A})}$ is the closure of $\Pi(\mathcal{A})$ in $\boldsymbol{R}^3$. Then the set $\overline{\Pi(\mathcal{C}_m^{\mathrm{J}})} \cap \partial_+ S_1^3$ consists of one (resp. two) point(s) if $\mathrm{J} = \mathrm{I}$ and m is odd (resp. if $\mathrm{J} = \mathrm{I}$ and m is even, or $\mathrm{J} = \mathrm{II}$). On the other hand, $\overline{\Pi(\mathcal{C}_m^{\mathrm{J}})} \cap \partial_- S_1^3$ always consists of two points, that is, the number of the endpoints of $\mathcal{C}_m^{\mathrm{J}}$ ($\mathrm{J} = \mathrm{I}, \mathrm{II}$) is three or four (cf. Theorems 4 and 6). This is a remarkable phenomenon, since other elliptic catenoids in S_1^3 do not have any analytic extensions and have exactly two endpoints.

2. Exceptional catenoids of type I.

In this section, we show that f_m^{I} has an analytic extension. For each integer $m \geq 2$, we set

$$f_m^{\mathrm{I}}(r,\theta) = \big(x_0(r,\theta), x_1(r,\theta), x_2(r,\theta), x_3(r,\theta)\big),$$

with $z = re^{\mathrm{i}\theta}$ ($r > 0$, $\theta \in S^1 := \boldsymbol{R}/2\pi\boldsymbol{Z}$). Then

$$x_0 \pm x_3 = \frac{m^2-1}{4m} r^{\pm 1}\left(2\cos m\theta - \frac{m \mp 1}{m \pm 1} r^m\right), \tag{6}$$

$$x_1 + \mathrm{i}x_2 = \frac{(m-1)^2}{4m} e^{\mathrm{i}(m+1)\theta} + \frac{(m+1)^2}{4m} e^{-\mathrm{i}(m-1)\theta} - e^{\mathrm{i}\theta}\frac{m^2-1}{4m} r^m. \tag{7}$$

We know that $f_m^{\mathrm{I}}(r,\theta)$ has self-intersections, since it contains swallowtail singularities (cf. Proposition A.1 in Appendix A). The limit curve

$$\gamma_m(\theta) := \lim_{r\to 0}(x_1, x_2) \tag{8}$$

gives a closed regular planar curve.

A *hypo-trochoid* is a roulette traced by a point attached to a disk of radius r_c rolling along the inside of a fixed circle of radius r_m, where the point is

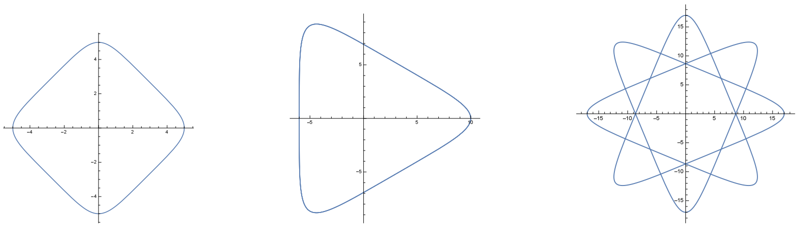

FIGURE 6. The trochoids for $m = 2, 3, 4$.

a distance d from the center of the interior circle. The parametrization of a hypo-trochoid is given by

$$x(s) = (r_c - r_m)\cos s + d\cos\left(\frac{r_c - r_m}{r_m}s\right),$$
$$y(s) = (r_c - r_m)\sin s - d\sin\left(\frac{r_c - r_m}{r_m}s\right).$$

We prove the following:

Proposition 1. *The plane curve $\gamma_m(\theta)$ has the following properties:*

(a) $\gamma_m(\theta+\pi) = (-1)^{m+1}\gamma_m(\theta)$ *for* $\theta \in \boldsymbol{R}$,
(b) *the image of* γ_m *is a convex curve if* $m = 2, 3$,
(c) γ_m *is a hypo-trochoid with (cf. Figure 6)*

$$r_c = \frac{m-1}{2}, \quad r_m = \frac{m^2-1}{4m}, \quad d = \frac{(m+1)^2}{4m}.$$

Proof. The first two assertions follow immediately. The last assertion follows from the expressions

$$x_1 = \frac{(m-1)^2\cos(m+1)\theta + (m+1)^2\cos(m-1)\theta}{4m},$$
$$x_2 = \frac{(m-1)^2\sin(m+1)\theta - (m+1)^2\sin(m-1)\theta}{4m}. \qquad \square$$

We set $\Omega := \Omega^+ \cup \Omega^-$, where

$$\Omega^\pm := \{(r,\theta) \in \boldsymbol{R}\times S^1\,;\, \pm r > 0\} \quad \big(S^1 := \boldsymbol{R}/2\pi\boldsymbol{Z}\big).$$

The expressions (6) and (7) are meaningful for $r < 0$ as well, and f_m^{I} can be extended to Ω. We denote this extension by $\tilde{f}_m^{\mathrm{I}} \colon \Omega \to S_1^3$. If m is odd, then

$$\tilde{f}_m^{\mathrm{I}}(-r, \theta+\pi) = \tilde{f}_m^{\mathrm{I}}(r,\theta). \tag{9}$$

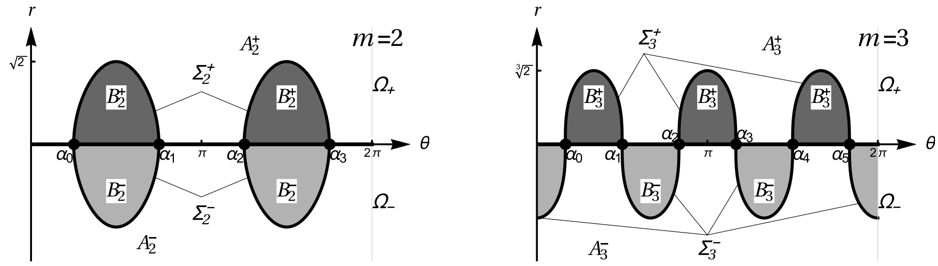

FIGURE 7. The domains of $\tilde{f}^{\mathrm{I}}_m$ and their singular sets.

In particular, if m is odd, the image of f^{I}_m coincides with that of $\tilde{f}^{\mathrm{I}}_m$. On the other hand, if m is even,

$$\tilde{f}^{\mathrm{I}}_m(-r,\theta) = \iota \circ \tilde{f}^{\mathrm{I}}_m(r,\theta),$$

where ι is the isometric involution given by

$$\iota\colon S^3_1 \ni (t,x,y,z) \mapsto (-t,x,y,-z) \in S^3_1. \tag{10}$$

Thus, if m is even, $f^{\mathrm{I}}_m(\Omega^+)$ and $f^{\mathrm{I}}_m(\Omega^-)$ are congruent, but do not coincide with each other. The singular set of $\tilde{f}^{\mathrm{I}}_m$ is $\Sigma_m := \Sigma^+_m \cup \Sigma^-_m$, where

$$\Sigma^{\pm}_m := \{(r,\theta) \in \Omega^{\pm}\,;\, r^m + 2\cos m\theta = 0\},$$

each of which consists of m components. The image of each component of the singular set is a curve with singularities which is bounded in S^3_1, whose endpoints are

$$P_k := \bigl(0, \gamma_m(\alpha_k), 0\bigr), \qquad \alpha_k := \frac{2k+1}{2m}\pi \qquad (k = 0,\dots,2m-1). \tag{11}$$

We denote by $A^{\pm}_m$ the domain in $\Omega^{\pm}$ containing a neighborhood of $r = \pm\infty$, and $B^{\pm}_m := \Omega^{\pm} \setminus \overline{A^{\pm}_m}$. Then we have the expressions

$$A^{\pm}_m = \{(r,\theta) \in \Omega^{\pm}\,;\, \epsilon^m(r^m + 2\cos m\theta) > 0\}, \tag{12}$$

$$B^{\pm}_m = \{(r,\theta) \in \Omega^{\pm}\,;\, \epsilon^m(r^m + 2\cos m\theta) < 0\}, \tag{13}$$

where ϵ is the sign of r (cf. Figure 7). We next consider the light-like lines

$$L_k := \{(t, \gamma_m(\alpha_k), -t)\,;\, t \in \boldsymbol{R}\} \subset S^3_1$$

passing through P_k for $k = 0,1,\dots,2m-1$, and set

$$\mathcal{C}^{\mathrm{I}}_m := \tilde{f}^{\mathrm{I}}_m(\Omega) \cup L_0 \cup \cdots \cup L_{2m-1}.$$

Then $\mathcal{C}^{\mathrm{I}}_m$ is the analytic extension of f^{I}_m. In fact,

Theorem 2. *For each integer $m \geq 2$,*

(i) $\mathcal{C}_m^{\mathrm{I}}$ *is a closed set of* S_1^3. *In particular, if* m *is odd, then* $\mathcal{C}_m^{\mathrm{I}}$ *is the closure of the image of* f_m^{I}. *On the other hand, if* m *is even, then the closure of the image of* f_m^{I} *is just half of* $\mathcal{C}_m^{\mathrm{I}}$. *The other half can be obtained by the isometric involution* ι *of* S_1^3 *given in* (10).

(ii) *Moreover,* $\mathcal{C}_m^{\mathrm{I}}$ *is analytically immersed outside the compact set consisting of the image of* Σ_m, *and the points* $\{(0, \gamma_m(\alpha_k), 0)\,;\, k = 0, \dots, 2m-1\}$.

Proof. By (6), $x_0(r, \theta)$ diverges for $r \to \pm\infty$. Take a sequence $\{\zeta_j = (r_j, \theta_j)\}_{j=1,2,\dots}$ on Ω such that $\lim_{j\to\infty} r_j = 0$. Taking a subsequence if necessary, we may assume $\{\zeta_j\}$ is included in Ω^+ or Ω^-, and $\lim_{j\to\infty} \theta_j = \beta$. If $\cos m\beta \neq 0$, (6) implies that $\lim_{j\to\infty} x_0(r_j, \theta_j)$ diverges. On the other hand, if $\cos m\beta = 0$, that is, $\beta = \alpha_k$ for some k, then $\lim_{j\to\infty}(x_0(\zeta_j) + x_3(\zeta_j))$ tends to 0, that is, $\tilde{f}_m^{\mathrm{I}}(\zeta_j)$ is asymptotic to the line L_k. Conversely, for each point $Q_{k,t} := (t, \gamma_m(\alpha_k), -t) \in L_k$, we set

$$\zeta_j := \left(\frac{1}{j}, \frac{1}{m}\cos^{-1}\frac{4mt}{j(m^2-1)}\right) \qquad (j = 1, 2, \dots),$$

where $\cos^{-1}$ is the inverse function of cos as a map

$$\cos^{-1}\colon (-1, 1) \to \left(m\alpha_k - \frac{\pi}{2}, m\alpha_k + \frac{\pi}{2}\right). \tag{14}$$

Then $\lim_{j\to\infty} \zeta_j = (0, \alpha_k)$ and $\lim_{j\to\infty} \tilde{f}_m^{\mathrm{I}}(\zeta_j) = Q_{k,t}$, where α_k is as in (11). Hence $\mathcal{C}_m^{\mathrm{I}}$ is the closure of the image of $\tilde{f}_m^{\mathrm{I}}$, proving the first part of (i). The second part of (i) is already proven. We next prove (ii). Since $\tilde{f}_m^{\mathrm{I}}$ is an analytic immersion on $\Omega \setminus \Sigma_m$, it is sufficient to show that $\mathcal{C}_m^{\mathrm{I}}$ is parametrized analytically on a neighborhood of L_k, which gives an immersion on $L_k \setminus \{P_k\}$. For this purpose, we set $s := (\cos m\theta)/r$. Then the x_j $(j = 0, 1, 2, 3)$ have the following expressions:

$$\begin{aligned} x_0 \pm x_3 &= \frac{m^2-1}{4m} r^{\pm 1}\left(2rs - \frac{m \mp 1}{m \pm 1} r^m\right), \\ x_1 + \mathrm{i}x_2 &= \frac{e^{\mathrm{i}\cos^{-1}(sr)/m}}{4m}\Big((m-1)^2 e^{\mathrm{i}\cos^{-1}(sr)} \\ &\qquad\qquad + (m+1)^2 e^{-\mathrm{i}\cos^{-1}(sr)}(m^2-1)r^m\Big). \end{aligned}$$

Since $\left(\partial(x_1 + \mathrm{i}x_2)/\partial r\right)\big|_{(0,s)} \neq 0$ if $s \neq 0$, one can easily check that $\tilde{f}_m^{\mathrm{I}}(r, s)$ is an immersion at $(0, s)$ for each $s \in \boldsymbol{R}\setminus\{0\}$, which proves the assertion. $\square$

Remark 3. For the parametrization (r,s) as in the proof of Theorem 2, the origin $(r,s)=(0,0)$ is a singular point for each $k=0,1,\dots,2m-1$, whose image is the point P_k given in (11). One can show that this parametrization gives a wave front on a neighborhood of $(0,0)$, and the origin is a cuspidal edge (resp. swallowtail) when $m=2$ (resp. $m=3$), see Appendix A.

Next, we consider the endpoints of $\mathcal{C}_m^{\mathrm{I}}$. Let

$$p_\pm := \bigl(0,0,\pm(\sqrt{2}-1)\bigr) \in \partial_+ S_1^3, \qquad n_\pm := \bigl(0,0,\pm(\sqrt{2}+1)\bigr) \in \partial_- S_1^3, \tag{15}$$

where $\partial_\pm S_1^3$ are the ideal boundaries given in (5). We set

$$y := (y_1,y_2,y_3) := \mathit{\Pi} \circ f_m^{\mathrm{I}} = \frac{1}{\delta}(x_1,x_2,x_3), \tag{16}$$

where $\delta = x_0 + \sqrt{2x_0^2+1}$ (cf. (1)).

Theorem 4. *If m is even (resp. odd), the set of endpoints of $\mathcal{C}_m^{\mathrm{I}}$ is $\{p_\pm, n_\pm\}$ (resp. $\{p_-, n_\pm\}$). More precisely, let $\{\zeta_j = (r_j,\theta_j)\}$ be a sequence in Ω whose image under $\tilde{f}_m^{\mathrm{I}}$ is unbounded. Then the following cases occur:*

1. *$\lim_{j\to\infty} y(\zeta_j) = n_-$ holds when $\lim_{j\to\infty} r_j = +\infty$ (that is, $\{\zeta_j\}$ lies in Ω^+ and diverges).*
2. *When $\lim_{j\to\infty} r_j = -\infty$, that is, if $\{\zeta_j\}$ lies in Ω^- and diverges, then $\lim_{j\to\infty} y(\zeta_j)$ is p_+ (resp. n_-) if m is even (resp. odd).*
3. *When $r_j \to 0$ and $\{\zeta_j\}$ is contained in A_m^+ (resp. A_m^-, B_m^+, B_m^-), the limit of $y(\zeta_j)$ is obtained as in the following table:*

The domain containing $\{\zeta_j\}$	A_m^+	A_m^-	B_m^+	B_m^-
$\lim_{j\to\infty} y(\zeta_j)$ *for even* m	p_-	n_+	n_+	p_-
$\lim_{j\to\infty} y(\zeta_j)$ *for odd* m	p_-	p_-	n_+	n_+

Proof. We rewrite (16) as

$$y_l = \frac{x_l/x_0}{1+\operatorname{sgn}(x_0)\sqrt{2+1/(x_0)^2}} \quad (l=1,2,3), \tag{17}$$

where $\operatorname{sgn}(x_0)$ denotes the sign of x_0. By (6) and (7),

$$\lim_{r\to\pm\infty} \frac{x_3}{x_0} = 1, \qquad \lim_{r\to\pm\infty} \frac{x_l}{x_0} = 0 \quad (l=1,2),$$
$$\lim_{r\to+\infty} x_0 = -\infty, \qquad \lim_{r\to-\infty} (-1)^m x_0 = \infty,$$

proving (1) and (2).

We prove (3) for the case that $\{\zeta_j\} \subset B_m^-$. Noticing that $r_j < 0$, (13) implies that

$$(-1)^m \left(r_j^{m-1} + \frac{\cos m\theta_j}{r_j} \right) > 0$$

holds for each j. Since $\{x_0(\zeta_j)\}$ is unbounded, so is $(\cos m\theta_j)/r_j$. Then the sign of $(\cos m\theta_j)/r_j$ is equal to $(-1)^m$ for sufficiently large j because r_j tends to 0. Then by (6), $\operatorname{sgn}\bigl(x_0(\zeta_j)\bigr) = (-1)^m$. On the other hand, (6) implies that $\lim_{j\to\infty} x_3(\zeta_j)/x_0(\zeta_j) = -1$. Thus, we have

$$\lim_{j\to\infty} y_3(\zeta_j) = \frac{-1}{1+(-1)^m\sqrt{2}} = 1 - (-1)^m\sqrt{2}.$$

Since x_1 and x_2 are bounded near $r = 0$, $y_l(\zeta_j)$ tends to 0 for $l = 1, 2$. Thus we have the conclusion. The other cases can be proved similarly. □

3. Exceptional catenoids of type II.

Here we show that the image of the exceptional catenoid f_m^{II} in S_1^3 has an analytic extension. For each integer $m \geq 2$, we set

$$f_m^{\mathrm{II}}(r,\theta) = \bigl(x_0(r,\theta), x_1(r,\theta), x_2(r,\theta), x_3(r,\theta)\bigr),$$

with $z = re^{\mathrm{i}\theta}$ ($r > 0$, $\theta \in [0, 2\pi)$). By (4), f_m^{II}'s components are

$$\begin{aligned} x_0 &= \frac{1-m^2}{4m}\left(r + \frac{1}{r}\right)\cos m\theta, \\ x_3 &= \frac{1-m^2}{4m}\left(r - \frac{1}{r}\right)\cos m\theta, \\ x_1 &= -\frac{(m^2+1)\cos m\theta\cos\theta + 2m\sin m\theta\sin\theta}{2m}, \\ x_2 &= -\frac{(m^2+1)\cos m\theta\sin\theta - 2m\sin m\theta\cos\theta}{2m}, \end{aligned} \tag{18}$$

where $z = re^{\mathrm{i}\theta}$ ($r > 0$, $\theta \in [0, 2\pi)$). The secondary Gauss map g_m of f_m^{II} is a meromorphic function on $\boldsymbol{C} \cup \{\infty\}$ given by (cf. [1, (39)])

$$g_m = (z^m - 1)/(z^m + 1).$$

Since the singular set Σ_m of the map f_m^{II} is

$$\Sigma_m = \{z \in \boldsymbol{C} \setminus \{0\}\,;\, |g_m(z)| = 1\} = \{re^{\mathrm{i}\theta} \in \boldsymbol{C} \setminus \{0\}\,;\, \cos m\theta = 0\},$$

we have $\Sigma_m = \sigma_0 \cup \sigma_1 \cup \cdots \cup \sigma_{2m-1}$, where

$$\sigma_k := \left\{z = re^{\mathrm{i}\alpha_k}\,;\, r > 0\right\} \quad \left(\alpha_k := \tfrac{(2k+1)\pi}{2m}\right) \tag{19}$$

for $k = 0, \dots, 2m-1$. In particular, if we set

$$\Omega_k := \left\{ re^{i\theta} \,;\, \tfrac{(2k-1)\pi}{2m} < \theta < \tfrac{(2k+1)\pi}{2m},\ r > 0 \right\}, \tag{20}$$

then the union of the Ω_k ($k = 0, \dots, 2m-1$) is the regular set of f_m^{II}, that is, the regular set consists of a disjoint union of $2m$ sectors.

Proposition 5. *The map f_m^{II} satisfies:*

(i) *For each $m \geq 2$, the image $f_m^{\mathrm{II}}(\sigma_k)$ consists of a point. More precisely,*

$$f_m^{\mathrm{II}}(\sigma_k) = (-1)^k (0, -\sin\alpha_k, \cos\alpha_k, 0),$$

where α_k is as in (19) *($k = 0, \dots, 2m-1$).*

(ii) *The endpoints of the image of f_m^{II} are the four points $p_\pm$ and $n_\pm$ as in* (15)*.*

Proof. Substituting $\theta = \alpha_k$ into (18) and using that $\cos m\theta = 0$ and $\sin m\theta = (-1)^k$ on σ_k, we get the first assertion.

To prove the second assertion, we remark that

$$\operatorname{sgn}(x_0) = (-1)^{k+1} \qquad (\text{on } \Omega_k), \tag{21}$$

for each k, since $\operatorname{sgn}(\cos m\theta) = (-1)^k$. Take a sequence $\{z_j\}$ on $\boldsymbol{C} \setminus \{0\}$ such that $\mathit{\Pi} \circ f_m^{\mathrm{II}}(z_j)$ converges to one of the points in the ideal boundary. By (i), we may assume that each $z_j \notin \Sigma_m$. With finitely many sectors, we may also assume $\{z_j\} \subset \Omega_k$ for some k. Then $x_0(z_j)$ diverges to ∞ or $-\infty$ as $j \to \infty$, that is, $\{r_j + r_j^{-1}\}_{j=1,2,\dots}$ is unbounded, where $r_j := |z_j|$. Taking a subsequence, we may assume

$$\lim_{j\to\infty} r_j = 0 \quad \text{or} \quad \lim_{j\to\infty} r_j = \infty. \tag{22}$$

We set $y := \mathit{\Pi} \circ f_m^{\mathrm{II}}$. Since x_1 and x_2 are bounded (cf. (18)), $y_l(z_j) \to 0$ for $l = 1, 2$, where $y = (y_1, y_2, y_3)$. On the other hand, by (18) and (22), we have $\lim_{j\to\infty} \bigl(x_3(z_j)/x_0(z_j)\bigr) = \pm 1$. Thus, we have $\lim_{j\to\infty} y_3(z_j) = \pm\sqrt{2} \pm 1$, which proves (ii). $\square$

It should be remarked that x_1, x_2 depend only on the variable θ, and

$$\bigl(x_1(\theta), x_2(\theta)\bigr) = -2\gamma_m(\theta)$$

holds. Here, γ_m is exactly the same hypo-trochoid as given in Proposition 1. For fixed θ, the image of the curve defined by $r \mapsto \bigl(x_0(r,\theta), x_3(r,\theta)\bigr)$ coincides with

$$\left\{ (t, z) \in \boldsymbol{R}_1^2 \,;\, t^2 - z^2 = \frac{(m^2-1)^2}{(2m)^2} \cos^2 m\theta,\ \operatorname{sgn}(\cos m\theta) t < 0 \right\}. \tag{23}$$

In particular, it is half of a hyperbola when $\cos m\theta \neq 0$. If $\cos m\theta = 0$, the image reduces to a point. So we can conclude that the real analytic extension of the image of f_m^{II} coincides with the set

$$\mathcal{C}_m^{\mathrm{II}} := \Big\{(t,x,y,z) \in \boldsymbol{R}_1^4\,;\, (x,y) = -2\gamma_m(\theta), \\ t^2 - z^2 = \frac{(m^2-1)^2}{(2m)^2}\cos^2 m\theta,\ \theta \in [0,2\pi)\Big\}.$$

For each $k = 0,\dots,2m-1$, the analytic extension $\mathcal{C}_m^{\mathrm{II}}$ contains a union of two light-like lines

$$L_k^{\pm} := \{(t, -\sin\alpha_k, \cos\alpha_k, \pm t)\,;\, t \in \boldsymbol{R}\},$$

where α_k is as in (19). Moreover, $\mathcal{C}_m^{\mathrm{II}}$ is symmetric with respect to the isometric involution

$$S_1^3 \ni (t,x,y,z) \longmapsto (t, \cos(2\alpha_k)x + \sin(2\alpha_k)y, \sin(2\alpha_k)x - \cos(2\alpha_k)y, z) \in S_1^3.$$

This involution fixes the two lines L_k^+ and L_k^-. Suppose that m is an odd integer. By (a) of Proposition 1, γ_m is π-periodic. In this case, one half of the hyperbola at $\theta + \pi$ is just the other half of the hyperbola (23) at θ, and $\mathcal{C}_m^{\mathrm{II}}$ coincides with the closure of the image of f_m^{II}.

In the case m is even, $\mathcal{C}_m^{\mathrm{II}}$ does not coincide with the closure of the image of f_m^{II}. Moreover, $\mathcal{C}_m^{\mathrm{II}}$ contains the image of the map $\iota\circ f_m^{\mathrm{II}}$, which is congruent to f_m^{II}, where ι is the involution as in (10), and $\mathcal{C}_m^{\mathrm{II}}$ is just the closure of the union of the images of f_m^{II} and $\tilde{f}_m^{\mathrm{II}}$. Figure 4 shows $\mathcal{C}_m^{\mathrm{II}}$ and the image of f_m^{II} for $m = 2$.

Summarizing the above, we get the following:

Theorem 6. *For each $m = 2,3,\dots$, the set $\mathcal{C}_m^{\mathrm{II}}$ gives the real analytic extension of the exceptional catenoid f_m^{II}, and has the following properties:*

(i) *The projection of $\mathcal{C}_m^{\mathrm{II}}$ into the xy-plane in $\boldsymbol{R}_1^4$ is the hypo-trochoid $-2\gamma_m$. Furthermore, the section of $\mathcal{C}_m^{\mathrm{II}}$ by a plane containing a point of the hypo-trochoid and perpendicular to the xy-plane is a hyperbola unless the plane passes through the cone-like singularity of $\mathcal{C}_m^{\mathrm{II}}$.*

(ii) *$\mathcal{C}_m^{\mathrm{II}}$ is almost immersed and has four endpoints. Two of them lie in $\partial_+S_1^3$ and the others lie in $\partial_-S_1^3$. Moreover, $\mathcal{C}_m^{\mathrm{II}}$ is almost embedded if $m = 2,3$.*

(iii) *If m is odd, then $\mathcal{C}_m^{\mathrm{II}}$ is the closure of the image of f_m^{II}. On the other hand, if m is even, then the closure of the image of f_m^{II} is just half of $\mathcal{C}_m^{\mathrm{II}}$. The other half can be obtained by the isometric involution of S_1^3 given in* (10).

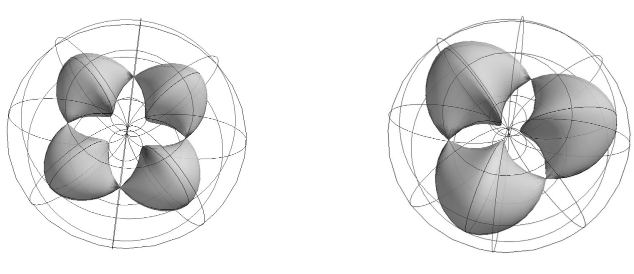

FIGURE 8. The images of $\check{f}_m$ for $m = 2$ (left) and $m = 3$ (right).

When $m \geq 4$, $\mathcal{C}_m^{\mathrm{II}}$ has self-intersections. It should be remarked that similar phenomena occur for parabolic or hyperbolic catenoids in the class of space-like maximal surfaces in $\boldsymbol{R}_1^3$ (see [3]).

Remark 7. As shown in [2], $\mathcal{C}_m^{\mathrm{II}}$ is analytically complete, that is, $\mathcal{C}_m^{\mathrm{II}}$ admits no analytic extension.

To end this paper, we remark that the replacement

$$s \mapsto \mathrm{i}s \qquad (r = e^s)$$

of the parameter of f_m^{II} induces constant mean curvature surfaces in anti-de Sitter space. This induces a family of surfaces

$$\check{f}_m := \big(x_0(s,\theta), x_1(\theta), x_2(\theta), x_3(s,\theta)\big)$$

given by $(x_0, x_3) = \frac{1-m^2}{2m}\cos m\theta\big(\cos s, \sin s\big)$, and x_1, x_2 as in (18), where $m = 2, 3, 4, \dots$. For each m, the corresponding surface lies in the space form

$$H_1^3(-1) := \{(t, x, y, z)\,;\, t^2 - x^2 - y^2 + z^2 = -1\}$$

of constant curvature -1 realized in $(\boldsymbol{R}_2^4, + - - +)$. The image of $\check{f}_m$ gives a compact almost immersed time-like surface of constant mean curvature one having a finite number of cone-like singularities. Moreover, if m equals 2 or 3, the surface is almost embedded in the sense given in the introduction. To draw the surfaces, we use the 'solid torus model' of $H_1^3(-1)$, that is, we define the following projection

$$\check{\Pi} : H_1^3(-1) \ni (t, x, y, z) \longmapsto \frac{1}{\rho}\left(\left(1 + \frac{t}{\rho}\right)x, \left(1 + \frac{t}{\rho}\right)y, z\right) \in \boldsymbol{R}^3,$$

where $\rho := \sqrt{x^2 + y^2}$. The image of $\check{\Pi}$ is the interior of the solid torus obtained by rotating the unit disk with center $(1, 0, 0)$ about the third axis in $\boldsymbol{R}^3$. The images of $\check{\Pi} \circ \check{f}_m$ for $m = 2, 3$ are given in Figure 8.

Appendix A. Singularities of Exceptional Catenoids of Type I

In this appendix, we discuss properties of singularities of the exceptional catenoids of type I. By the criteria in [5, Theorem 3.4], we have the following:

Proposition A.1. *The singular set of f_m^I is*

$$\Sigma_m := \{z = re^{\mathrm{i}\theta} \in \boldsymbol{C} \setminus \{0\}\,;\, r^m + 2\cos m\theta = 0\}.$$

The m points

$$z = re^{\mathrm{i}\theta}, \qquad (r,\theta) = \left(2^{1/m}, \frac{1}{m}(2j+1)\pi\right), \quad (j = 0,\dots,m-1)$$

are swallowtails, and the $2m$ points

$$z = re^{\mathrm{i}\theta}, \qquad (r,\theta) = \begin{cases} \left(2^{1/(2m)}, \frac{1}{m}\left(\frac{3}{4}+2j\right)\pi\right) \\ \left(2^{1/(2m)}, \frac{1}{m}\left(\frac{5}{4}+2j\right)\pi\right), \end{cases} \quad (j = 0,\dots,m-1)$$

are cuspidal cross caps. Other points in Σ_m are cuspidal edges.

Next, we discuss singularities of the parametrization of $\mathcal{C}_m^{\mathrm{I}}$ near the line L_k $(k = 0,\dots,2m-1)$, as in the proof of Theorem 2. Without loss of generality, we may assume $k = 0$. Then the parametrization is expressed as

$$\hat{f}_m^{\mathrm{I}}(r,s) := \bigl(x_0(r,s), x_1(r,s), x_2(r,s), x_3(r,s)\bigr),$$

where

$$\begin{aligned} x_0 + x_3 &:= \frac{m^2-1}{4m}\left(2r^2 s - \frac{m-1}{m+1} r^{m+1}\right), \\ x_0 - x_3 &:= \frac{m^2-1}{4m}\left(2s - \frac{m+1}{m-1} r^{m-1}\right), \\ x_1 + \mathrm{i}x_2 &:= \frac{(m-1)^2}{4m} e^{\mathrm{i}(m+1)\theta} + \frac{(m+1)^2}{4m} e^{-\mathrm{i}(m-1)\theta} - \frac{m^2-1}{4m} r^m e^{\mathrm{i}\theta} \end{aligned} \tag{A.24}$$

and

$$\theta := \theta(r,s) = \frac{1}{m}\cos^{-1}(rs), \tag{A.25}$$

where we consider $\cos^{-1}(rs) \in [0,\pi]$. As shown in Theorem 2, the map $\hat{f}_m^{\mathrm{I}}$ is an immersion at $(0,s)$ if $s \neq 0$. We show the following:

Proposition A.2. *The map $\hat{f}_m^{\mathrm{I}}$ is a wave front near the origin, and the origin* $(0,0)$ *is a cuspidal edge* (*resp. swallowtail*) *when* $m = 2$ (*resp.* $m = 3$).

Proof. Since

$$x_1(0,0) + \mathrm{i}x_2(0,0) = -\mathrm{i}e^{\mathrm{i}\pi/(2m)} = \sin\frac{\pi}{2m} - \mathrm{i}\cos\frac{\pi}{2m},$$

$x_1(0,0) \neq 0$. Then

$$\pi\colon S^3_1 \ni (x_0, x_1, x_2, x_3) \mapsto (x_0 + x_3, x_0 - x_3, x_1) \in \boldsymbol{R}^3$$

gives a local coordinate system of S^3_1 around $\hat{f}^{\mathrm{I}}_m(0,0)$. So it is sufficient show the conclusion for the map

$$F(r,s) := \pi \circ \hat{f}^{\mathrm{I}}_m(r,s) = \bigl(X(r,s), Y(r,s), Z(r,s)\bigr), \tag{A.26}$$

where

$$\begin{aligned} X(r,s) &:= 2(m+1)r^2 s - (m-1)r^{m+1},\\ Y(r,s) &:= 2(m-1)s - (m+1)r^{m-1},\\ Z(r,s) &:= \frac{m-1}{m+1}\cos(m+1)\theta + \frac{m+1}{m-1}\cos(m-1)\theta - r^m\cos\theta. \end{aligned}$$

By (A.25),

$$\theta_r = -\delta s, \qquad \theta_s = -\delta r \qquad \left(\delta(r,s) := \frac{1}{m\sin m\theta(r,s)}\right)$$

hold. Then we have

$$\begin{aligned} F_r = \bigl(&(m+1)r(4s-(m-1)r^{m-1}), -(m^2-1)r^{m-2},\\ &(2s - mr^{m-1})\cos\theta - sr\delta\lambda\sin\theta\bigr),\\ F_s = \bigl(&2(m+1)r^2, 2(m-1), 2r\cos\theta - r^2\delta\lambda\sin\theta\bigr), \end{aligned}$$

where

$$\lambda := 2s + r^{m-1}. \tag{A.27}$$

By a direct computation, we have $F_r \times F_s = \lambda\nu$, where

$$\begin{aligned} \nu &:= (\nu_1, \nu_2, \nu_3)\\ \nu_1 &:= -(m-1)\bigl(2\cos\theta - r\delta(2s + (m+1)r^{m-1})\sin\theta\bigr),\\ \nu_2 &:= -(m+1)r^2\bigl(2\cos\theta - r\delta(2s - (m-1)r^{m-1})\sin\theta\bigr),\\ \nu_3 &:= 4(m^2-1)r. \end{aligned} \tag{A.28}$$

Since

$$\nu(0,0) = (-2(m-1)\cos(\pi/(2m)), 0, 0) \neq 0,$$

ν is the normal vector field of F, and λ in (A.27) is an identifier of singularities, that is, $\{(r,s)\,;\,\lambda(r,s)=0\}$ is the singular set. Since $d\lambda \neq 0$, the singular points of F are non-degenerate. Thus, the singular direction is

$$\xi := -2\frac{\partial}{\partial r} + (m-1)r^{m-2}\frac{\partial}{\partial s}. \tag{A.29}$$

On other hand, since $2F_r + (m+1)r^{m-2}F_s = \mathbf{0}$ when $\lambda(r,s) = 0$,

$$\eta := 2\frac{\partial}{\partial r} + (m+1)r^{m-2}\frac{\partial}{\partial s} \tag{A.30}$$

is the null direction. Moreover,

$$d\nu(\eta)(0,0) = (0,0,4(m^2-1)),$$

which is not proportional to $\nu(0,0)$. Thus, the map F gives a wave front near the origin.

When $m = 2$, the singular direction and the null direction are linearly independent at the origin. Hence, by the criterion in [6, Proposition 1.3], the origin is a cuspidal edge.

Finally, when $m = 3$, the singular direction and the null direction are

$$\xi = -2\frac{\partial}{\partial r} + 2r\frac{\partial}{\partial s}, \qquad \eta = 2\frac{\partial}{\partial r} + 4r\frac{\partial}{\partial s},$$

which are proportional at the origin. Moreover, $\det(\xi,\eta) = -12r$, where det is the determinant function on the (r,s)-plane. Hence by the criterion in [6, Proposition 1.3], the origin is a swallowtail. □

Acknowledgements. Fujimori was partially supported by the Grant-in-Aid for Scientific Research (C) No. 17K05219, Kawakami by (C) No. 15K04840, Kokubu by (C) No. 17K05227, Rossman by (C) No. 15K04845, Umehara by (A) No. 26247005, and Yamada by (B) No. 17H0282.

References

[1] S. Fujimori, Y. Kawakami, M. Kokubu, W. Rossman, M. Umehara and K. Yamada, *Hyperbolic metrics on Riemann surfaces and space-like CMC-1 surfaces in de Sitter 3-space*, M. Sánchez et al (eds.), Recent Trends in Lorentzian Geometry, Springer Proceedings in Mathematics & Statistics **26**, (2013), 1–47.

[2] S. Fujimori, Y. Kawakami, M. Kokubu, W. Rossman, M. Umehara, K. Yamada and S.-D. Yang, *Criteria for analytic completeness and application to constant mean curvature surfaces in de Sitter 3-space*, in preparation.

[3] S. Fujimori, Y. W. Kim, S.-E. Koh, W. Rossman, H. Shin, M. Umehara, K. Yamada and S.-D. Yang, *Zero mean curvature surfaces in Lorentz-Minkowski 3-space and 2-dimensional fluid mechanics*, Math. J. Okayama Univ. **57** (2015), 173–200.

[4] S. Fujimori, M. Noro, K. Saji, T. Sasaki and M. Yoshida, *Schwarz maps for the hypergeometric differential equation*, Internat. J. Math. **26** (2015), 1541002, 31pp.

[5] S. Fujimori, K. Saji, M. Umehara and K. Yamada, *Singularities of maximal surfaces*, Math. Z. **259** (2008), 827–848.

[6] M. Kokubu, W. Rossman, K. Saji, M. Umehara and K. Yamada, *Singularities of flat fronts in hyperbolic space*, Pacific J. Math. **221** (2005), 303–351, DOI: 10.2140/pjm.2018.294.505, Addendum: *Singularities of flat fronts in hyperbolic space*, Pacific J. Math. **294** (2018), 505–509.

Shoichi Fujimori
Department of Mathematics, Hiroshima University, Higashihiroshima 739-8526, Japan.
e-mail address: fujimori@hiroshima-u.ac.jp

Yu Kawakami
Graduate School of Natural Science and Technology, Kanazawa University, Kanazawa, 920-1192, Japan.
e-mail address: y-kwkami@se.kanazawa-u.ac.jp

Masatoshi Kokubu
Department of Mathematics, School of Engineering, Tokyo Denki University, Tokyo 120-8551, Japan.
e-mail address: kokubu@cck.dendai.ac.jp

Wayne Rossman
Department of Mathematics, Faculty of Science, Kobe University, Rokko, Kobe 657-8501, Japan.
e-mail address: wayne@math.kobe-u.ac.jp

Masaaki Umehara
Department of Mathematical and Computing Sciences, Tokyo Institute of Technology, 2-12-1-W8-34, O-okayama Meguro-ku, Tokyo 152-8552, Japan.
e-mail address: umehara@is.titech.ac.jp

Kotaro Yamada
Department of Mathematics, Tokyo Institute of Technology, Tokyo 152-8551, Japan.
e-mail address: kotaro@math.titech.ac.jp

(*Received July 7, 2018*)
(*Accepted December 17, 2018*)